Desalination and Water Treatment
www.deswater.com

doi:10.5004/dwt.2018.22033

111 (2018) 134–145
April

Impact of UV disinfection combined with chlorination on bacterial community structure and the formation of trihalomethanes in drinking water

Yulong Yang, Weien Jing, Kejia Zhang, Jingguo Zhao, Cong Li*, Xiaoyan Ma

College of Civil Engineering and Architecture, Zhejiang University, Hangzhou, 310058, China, email: yulongy@zju.edu.cn (Y. Yang), 21512164@zju.edu.cn (W. Jing), zhangkj@zju.edu.cn (K. Zhang), zhao0538@126.com (J. Zhao), congil@zju.edu.cn (C. Li), mayaner620@163.com (X. Ma)

Received 23 October 2017; Accepted 10 February 2018

ABSTRACT

The objective of this study was to evaluate the performance of the UV disinfection combined with chlorination in the inactivation of microorganisms and the formation of trihalomethanes (THMs). Experimental results showed that UV irradiation had obvious advantages in reducing the number of microbial species and community complexity. Under the same initial chlorine concentration, the amount of THMs increased with the UV radiation dose increasing. THMs will be reduced in the UV-chlorine disinfection process compared with the pure chlorine disinfection. In terms of number of surviving microorganisms in water, compared with a single chlorine disinfection, UV irradiation showed a very good disinfection effect. With an average 52.5% decline, the data reflected the sample after UV irradiation in microbial diversity and abundance significantly decreased. the physical and chemical properties of organic matter could be qualitatively and quantitatively described by 3DEEM.

Keywords: Ultraviolet treatment; Chlorination; Bacterial community structure; Trihalomethanes (THMs); Three dimensional excitation-emission matrix (3DEEM) diagram

1. **Introduction**

As a kind of high efficiency and low cost of disinfectant, chlorine is commonly used to destroy microorganisms and provide secondary disinfection in water supply networks. However, disinfection by-products (DBPs) produced in the process of chlorine disinfection is a great threat to human health [1]. Chlorine reacts with organic matter in water to produce DBPs. A pathological study has shown that the DBPs of chlorine disinfection in tap water has a certain relationship with the incidence of bladder cancer [2]. THMs and haloacetic acids (HAAs) are the two main types of DBPs, which are currently serious threat to human health [3]. Many studies have found that UV radiation can change the characteristics of organic matter in water, including reducing the concentration of organic matter, its color, as well as its molecular size [4].

The application of UV radiation can significantly reduce the concentration of disinfectant in the water treatment process [5]. UV radiation can efficiently kill cryptosporidium which has a strong resistance to chlorine [6]. It also minimizes water odor [7]. Some research results show the laboratory ultraviolet disinfection can not show the same disinfection effect in the actual production because of the complexity of the actual water environment, and larger doses of disinfection required [8]. Some researchers found that the effect on the production of THMs and HAAs is not obvious with the UV intensity of 40~186 mJ/cm^2 [9]. UV irradiation significantly increased chlorine demand and potential formation of THMs , which was different from expectations that UV disinfection will reduce the chlorine dosage and DBPs generation. The changes of HAAs formation was not obvious in water treated by UV combined with chlorine, but the concentration of absorbable organic halogen,chloral hydrate, THMs, dichloroacetonitrile (dichloroacetonitrile), 1,1,1-trichloropropanone and chloropicrin significantly increased [10].

*Corresponding author.

The present drinking water treatment technology cannot completely kill all bacteria in water, and disinfectants would have an impact on the microbial community structure in the downstream water [11]. In the previous joint disinfection, research focused on the *E. coli* [12] and other typical microorganisms [13,14], but not on the overall microbial community structure in water samples. In contrast, targeting at 16S rDNA, the DNA sequencing technology [15] were rapidly developed without culture, and the detection process has been gradually applied in the identification of microbial communities. The process could show the advantages of high-throughput sequencing of large data, and detect the abundance of as low as 1/10000 of trace bacteria, which shows a better effect on the detection of trace bacteria. In the pretreatment process, propidium monoazide (PMA) can selectively label DNA of dead cells exposed, so that it cannot be used for PCR amplification, which can achieve different phenomenon of total bacteria and live bacteria in water samples [16].

But no detailed study have been reported to describe the performance of the UV combined with chlorination in the inactivation of microorganisms and the formation of THMs. In this study, we used PMA treatment coupled with 454-pyrosequencing (PMA-pyrosequencing) targeting the 16S rRNA gene to study the dynamics of complex bacterial communities under UV radiation or chlorination disinfection in water samples collected from the pilot-scale drinking water treatment plant. Therefore, the main objective of this study was to investigate (i) the change of the bacterial community structure and the inactivation of microorganisms under UV radiation or chlorination disinfection through the advanced high-throughput MiSeq pyrosequencing. (ii) the formation of commom DBPs (THMs) in the water treated by UV and chlorination. (iii) the changes of water quality treated by UV and chlorination. Overall, the work presented in this study could assist in evaluating the disinfection efficiency of combined UV-chlorine process in drinking water treatment systems.

2. Materials and methods

2.1. Samples

The filtered water samples were taken from the pilot plant and stored refrigerator below 4°C. The water quality is shown in Supplementary Table S1. The pH of the test water sample was adjusted by dilute HCl and NaOH solution, and the chlorine was from a NaClO stock solution (50 mg/L).

2.2. UV disinfection device

The industrial and enclosed cylinder made of stainless steel with a UV lamp (PHILIPS) as the UV disinfection reactor was used in the experiments. The inner wall of the cylinder body is polished to enhance the ability of reflection and the intensity of ultraviolet radiation. The cylinder with a 12 cm diameter and a 90 cm length, can hold a large amount of water for continuous process. In order to improve the stability of operation and prevent organic and biological slime attaching to the UV lamp, there are two high transmittance quartz tubes outside of the lamp. An automatic cleaning device was installed for regular cleaning, removing residues, preventing water pollution, recovering UV transmittance to insure the disinfection effect. The power of the UV lamp is 40 W, the output wavelength is 254 nm. The UV intensity at the wall of the cavity is about 900 μw /cm^2. The UV disinfection device is shown in Supplementary Fig. S1.

2.3. UV disinfection experiments

The exposure time can be used to control the disinfection dosage. The filtered water sample was added into the UV disinfection device under different UV irradiation including , 0 mJ/cm^2, 27 mJ/cm^2, 54 mJ/cm^2, 270 mJ/cm^2, 540 mJ/cm^2, and 1620 mJ/cm^2. The samples by UV irradiation were added in beakers and different volumes of NaClO stock solution were added to adjust initial chlorine concentrations: 1.2 mg/L, 2.0 mg/L, 2.8 mg/L, and 3.6 mg/L. Then samples were mixed at 300 r/min by a thermostat blender at different sampling time (0.5 h, 1 h, 3 h, 5 h, 10 h, and 24 h). After reaction for 24 h, 0.1 mol/L of $Na_2S_2O_3$ solution was added into the samples to quench the chlorination, water samples were taken and transferred to head space-free amber glass bottles with caps and PTFE-lined septa and held at 4°C until concentration of THMs could be analyzed.

To compare the impact of a single disinfectant, i.e., UV only or chlorine only, on the bacterial community structure in drinking water systems, a range of disinfectant doses were added to the water, which was then investigated using high-throughput MiSeq pyrosequencing.

2.4. Analytical methods

Free Cl_2 was measured using the DPD colorimetric method by a Hach DR2800 analyser (HACH, USA). UV scanning at 254 nm was with a UV-visible spectrophotometer (Shimadzu, DR1800). To evaluate the structure changing of NOM after UV irradiation, the samples were scanned by UV-visible spectrophotometer and fluorescence excitation–emission (EEM) analysis (F-4500).

THMs were analyzed with a gas chromatograph (Varian, 450-GC) equipped with an electron capture detector (ECD) and the TEKMAR Atomx auto sampler, based on USEPA method 551.1. A DB-5 capillary column (30 m × 0.25 mm × 0.25 μm, Agilent) was used. The injector temperature was set at 150°C with splitless mode as follows: an initial temperature of 60°C for 5 min, ramping to 160°C at 10°C min^{-1}, and then ramping to 220°C at 20°C min^{-1} and holding for 2 min. The electron capture detector was set at 300°C, while the column flow was set at 1.0 mL/min. The 1, 2-dibromopropane was used as an internal standard in the tests with the accuracy measured as mean percent recovery (MPR) and the precision expressed as percent relative standard deviation (%RSD) in the determination of THMs by head space gas chromatography. Each sample was analyzed in triplicate. High accuracy and precision in the THMs determination was obtained, and the results were shown in Supplementary Table S2.

2.5. Biological indicator detection

High throughput sequencing is an analysis of the composition of the microbial population in a specific envi-

ronment or the composition and function of the gene by analyzing the composition of the sequence. The specific operation process includes the following steps:

2.5.1. Propidium monoazide (PMA) pretreatment

PMA is a photosensitive dye with high affinity to DNA. It can enter the dead cells, which cell wall or cell membrane was destroyed, and then selectively modify DNA molecules exposed, which could block DNA polymerase chain reaction (PCR), so as to distinguish between viable and dead bacteria. The sequencing results reflect the situation of live bacteria in the water after PMA treatment, and the results of sequencing in non-PMA of water samples treated reflect the total bacteria. PMA (Catalog# 40019, Biotium, Inc., Hayward, CA) was dissolved in 20% dimethyl sulfoxide to create a stock concentration of 20 mM and stored at –20°C in the dark. The water samples (2 L) after potassium ferrate and chlorine inactivation experiments were pelleted by centrifugation at 5000 g, washed and then resuspended in 10 mM PBS, and each split into two aliquots. Typically, 1.25 µL of PMA was added to one of the aliquots (500-µL each) to final concentrations of 50 µM, while the other aliquot served as a control. Light-transparent 1.5-ml microcentrifuge tubes were used. The samples were incubated in the dark for 15 min at room temperature, followed by light exposure for 10 min at a distance of 20 cm from a 650-W halogen light source (Sachtler R651HS; Camera Dynamics, Inc., Valley Cottage, NY). After photo-induced cross-linking, cells were collected at 5,000 × g for 5 min and stored at –80°C prior to DNA extraction. The samples of sand-filtered water subjected to chlorine disinfection (1.2 mg/L, 2.0 mg/L, 2.8 mg/L, and 3.6 mg/L) and UV disinfection (27 mJ/cm^2, 54 mJ/cm^2, 270 mJ/cm^2, and 540 mJ/cm^2) were named as Filter, Cl-1, Cl-2, Cl-3, Cl-4, UV-1, UV-2, UV-3, UV-4, respectively. The samples after the PMA treatment were named as Filter-P, Cl-1-P, Cl-2-P, Cl-3-P, Cl-4-P, UV-1-P, UV-2-P, UV-3-P, UV-4-P, respectively.

2.5.2. DNA extraction

About 5 L each of the sand-filtered water subjected to chlorine disinfection and UV disinfection were collected for DNA extraction. Each sample was filtered with 0.22 µm polycarbonate membranes (Whatman, Maidstone, UK) to collect the biomass. Genomic DNA of the above described samples, together with the PMA-treated samples, was extracted using an E.Z.N.A.® Water DNA kit (Omega Bio-Tek, Norcross, USA) following the manufacturer's instructions. The extracted nucleic acids were kept at –80°C until use.

2.5.3. PCR amplification

For PCR amplification, barcodes that allow sample multiplexing during pyrosequencing were incorporated in the primers 338F (ACTCCTACGGGAGGCAGCA) and 806R (GGACTACHVGGGTWTCTAAT). It was performed in triplicate using a Gene Amp PCR-System® 9700 (Applied Biosystems, Foster City, CA, USA) with a total volume of 20 µL containing 4 µL of 5× FastPfu buffer, 250 µmol/L of dNTPs, 0.8 µL of each 5 µmol/L primer, 0.4 µL FastPfu polymerase (TransGen Biotech, China) and 10 ng of DNA template. Thermal cycling conditions were as follows: an initial denaturation at 94°C for 2 min, and 32 cycles at 95°C for 30 s, 55°C for 30 s, and 72°C for 45 s, with a final extension at 72°C for 10 min and then were kept at 4°C. Following amplification, PCR products of the same sample were mixed uniformly and then the product was detected by 2% agarose gel electrophoresis. PCR products were recycled by gel Recovery Kit (AxyPrepDNA AXYGEN) and a TRis-HCl buffer solution was used for elution, followed by 2% agarose gel electrophoresis. The products were quantified using the QuantiFluor™ (Promega, Milano, Italy). The pyrosequencing was performed on the Illumina MiSeq platform by Majorbio Bio-Pharm Technology Co., Ltd. (Shanghai, China).

2.5.4. Sequencing data processing

Representative OTUs were selected based on the most abundant sequences in the samples and the Ribosomal Database Project (RDP) classifier was used for taxonomic assignments [17]. Additionally, the shared OTUs were used to estimate similarity between communities based on membership and structure. Mothur software [18] was used to generate the rarefaction curve and distance matrices, as well as to calculate richness estimators and diversity index including abundance-based coverage estimator (ACE), Chao1 richness estimator and Shannon diversity index. The Venn diagram with shared and unique OTUs was used to depict the similarity and difference among the bacterial communities. The Venn diagram used the R package (http:// www.r-project.org/).

3. Results and discussion

3.1. Sequence diversity analysis

Bacterial community structure for the water samples by UV and chlorine disinfection were monitored using PMA-pyrosequencing (PMA-treated samples to determine the live bacterial community), and pyrosequencing without PMA treatment was conducted as the control (no-PMA samples to determine the total bacterial community). Pyrosequencing yielded a total of 475,679 high-quality sequences of the 16S rRNA gene for all samples, among them 246,799 sequences were obtained for live bacteria (Table 1). Based on the clustering of these sequences at 97% gene similarity, 419 OTUs of live bacteria was found in the sand filter water sample, while 493, 400, 363, and 525 OTUs were found in the SF-Water by chlorine disinfection with the dose of 1.2 mg/L, 2.0 mg/L, 2.8 mg/L, and 3.6 mg/L, respectively. Meanwhile, 243, 252, 216 and 135 OTUs were found in the SF-Water by UV disinfection with a dose of 27 mJ/cm^2, 54 mJ/cm^2, 270 mJ/cm^2, and 540 mJ/cm^2, respectively (Table 1). In terms of the number of surviving microorganisms in water, compared with a single chlorine disinfection, UV irradiation showed a very good disinfection effect. With an average 52.5% decrease, the data reflected the sample after UV irradiation in microbial diversity and abundance significantly decreased. The ACE, Chao, Shannon, and

Table 1
Observed OTUs and α-diversity indexes of the live bacterial phylotypes in the samples

Sample ID	Reads	0.97					
		OTUs	ACE	Chao	Coverage	Shannon	Simpson
Filter	22598	384	466	459	99.6%	4.04	0.0437
Filter-P	18315	419	494	475	99.5%	4.01	0.0458
Cl-1	29667	413	523	522	99.6%	3.79	0.0474
Cl-2	17388	326	424	438	99.5%	3.69	0.0637
Cl-3	33658	400	518	522	99.7%	3.09	0.1254
Cl-4	18937	467	565	572	99.4%	3.98	0.0676
Cl-1-P	35279	493	557	569	99.7%	4.07	0.0394
Cl-2-P	29287	400	518	522	99.7%	3.09	0.1254
Cl-3-P	23525	363	487	485	99.5%	3.4	0.0737
Cl-4-P	35624	525	592	588	99.7%	3.84	0.0621
UV-1	32580	407	645	545	99.6%	2.95	0.1751
UV-2	26889	266	352	348	99.7%	3.4	0.0721
UV-3	16733	183	235	257	99.7%	2.9	0.1212
UV-4	30430	320	384	378	99.8%	2.85	0.1392
UV-1-P	28416	243	390	338	99.7%	1.88	0.4236
UV-2-P	26678	252	297	307	99.8%	3.48	0.075
UV-3-P	27193	216	270	309	99.8%	2.86	0.1274
UV-4-P	22482	135	180	182	99.8%	2.62	0.1312

[a]Trimmed reads that passed quality control; [b]The operational taxonomic units (OTUs) were determined with a 3% width; [c]ACE richness estimates; [d]chao1 richness estimates.

Simpson analysis show that the OTUs richness and bacteria diversity of the live bacteria is regular with the varying of disinfection dosages or type of disinfectant. The parameter values in water samples were obviously decreased after UV exposure, except for the Simpson index. The observed OTUs and α-diversity indexes for both live and total bacteria in all the samples are shown in Table 1. Shannon index is used to estimate the microbial diversity index in the sample, the greater the number, the lower the diversity of the community. For PMA-treated samples of water treated by chlorine, with a Shannon value range of 3.09~4.07, its mean is 3.60. Regarding water treated by UV, the Shannon value range was 1.88~3.48, and the mean is 2.71. Compared with chlorine disinfection, a water microbial community diversity decreasing with Shannon value decreasing 24.7%, UV disinfection showed a better disinfection effect.

3.2. Bacterial community and composition

The structure of the bacterial community at different taxonomic levels was provided for all samples. At class level (supplementary Table S3), the dominant viable bacteria in the samples include *Betaproteobacteria* (37.24%–96.54%), *Alphaproteobacteria* (3.02%–47.83%), *Flavobacteria* (0.08%–9.14%), *Gammaproteobacteria* (0.13%–21.81%) and *Sphingobacteriia* (0.03%–5.54%), with other minor classes belonging to *Actinobacteria* (0.08%–2.54%), *Acidobacteria* (0.02%–2.41%), *Deltaproteobacteria* (0.00%–1.70%), and. The bacterial community composition is irregular with the varying dosages for the same changes in the relative abundance of these OTUs. There were significant differences in the dominant species in each water sample. Generally, the microbial community of the samples was dominated by *Novosphingobium*, *Polynucleobacter*, *Duganella*, *Flavobacterium*, *Sphingobium*, *Herminiimonas*, and *Limnohabitans*. The relative abundance of these OTUs was different drastically among each individual sample. After ultraviolet disinfection, the dominant species in water samples decreased significantly. As shown in Fig. 1, after PMA treatment, the relative abundance of OTUs more than 4% was 9 in sand filter water, 8 after 3.6 mg/L chlorine disinfection, but 4 after a 27 mJ/cm^2 dose of UV irradiation. These mean that UV radiation can achieve the same effect of high concentration of chlorine to kill microbials under the lower dosages of ultraviolet,. The changes in dominant OTUs suggest that different populations exhibit variable levels of chlorine or UV resistance.

The molecular analysis in this study distinguished the dead and viable microbial populations and suggested that different disinfection modes of chlorine and UV likely played a major role in shaping the corresponding differences in the structure of microbial communities.

3.3. Influence of UV dose on the formation of THMs

The formation of THMs increased with the increasing of UV irradiation under the same initial chlorine concentration (Fig. 2). And the general process can be divided into three stages: water samples without UV (0 mJ/cm^2), water samples with low UV irradiation（27 mJ/cm^2~54 mJ/cm^2.）and water samples with high UV irradiation (270 mJ/cm^2~1620 mJ/cm^2). When the initial chlorine con-

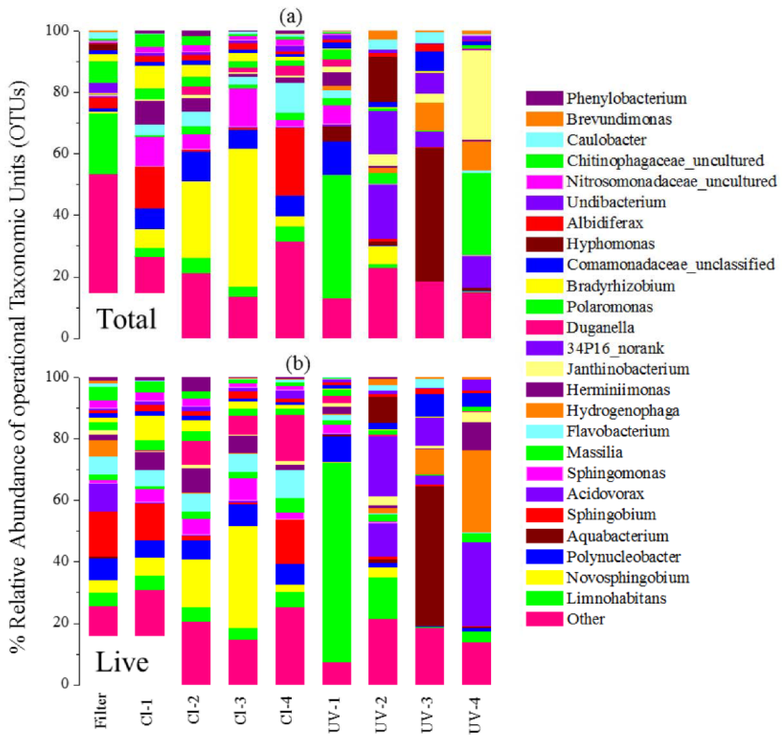

Fig. 1. Relative abundance of OTUs represented by their taxonomic group for water samples after sand filtration, chlorine disinfection, and UV disinfection showing total bacteria (no PMA) (a) and the live fraction (PMA) (b). The 25 most abundant OTUs for all samples combined are listed, whereas all other OTUs were combined and are shown as "other".

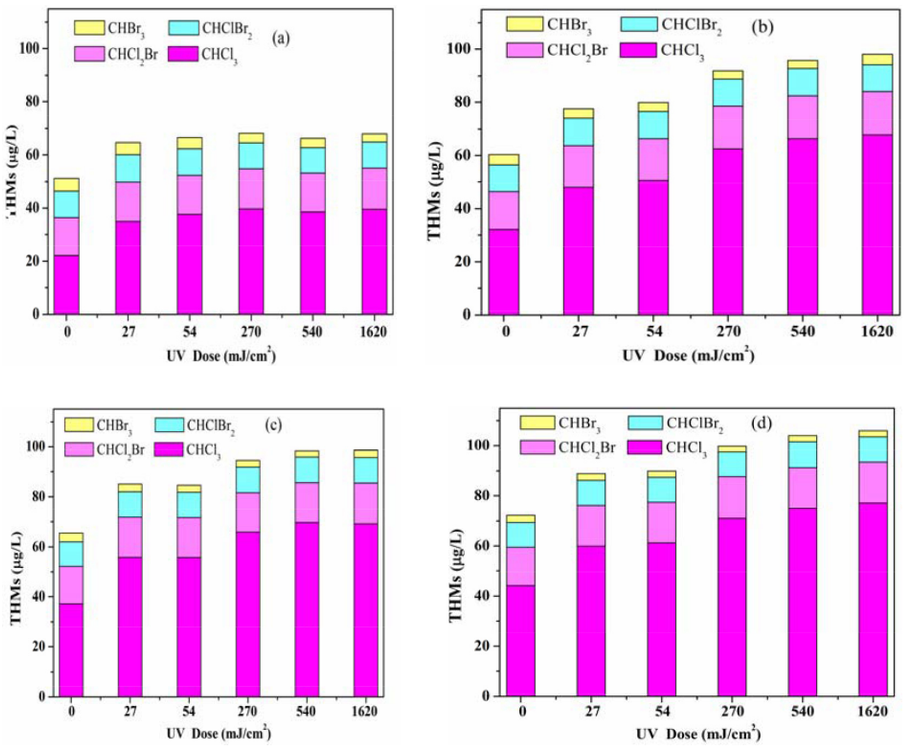

Fig. 2. Influence of UV dose on the formation of THMs: (a) Cl_0 = 1.2 mg/L; (b) Cl_0 = 2.0 mg/L; (c) Cl_0 = 2.8 mg/L; (d) Cl_0 = 3.6 mg/L.

centration was 2.0 mg/L and 2.8 mg/L, the concentration of THMs in the untreated water samples were 60.3 μg/L and 65.5 μg/L, respectively. The average concentrations of THMs in the water samples with low dose irradiation were 78.7 μg/L and 84.9 μg/L, respectively, and increased 30.5% and 29.6% compared with untreated water sample. The average concentrations of THMs in samples with high doses were 95.2 μg/L and 97.1 μg/L, respectively, with the increase of 57.9% and 48.2% compared with untreated water sample. It can be seen that the main change of the concentration of THMs under different conditions is $CHCl_3$, and the change of other components concentration is not obvious. The concentration of $CHCl_3$ in untreated water samples was 22.2 μg/L with the initial chlorine concentration of 1.2 mg/L, accounting for 43.4% of THMs.

The combination disinfection process of UV and chlorine had been studied where the formation of THMs, HAAs, and haloacetonitriles would increase in the water sample after UV treatment followed by same chlorination compared with only chlorine disinfection [9,19]. In this study, combined with the conclusions of microorganisms research, the disinfection effect of microorganisms at the chlorine concentration of 3.6 mg/L can reach at 27 mJ/cm^2 UV dosage of 27 mJ/cm^2. The more the UV dosage increased, the better the disinfection reached. It can be speculated that the usage of UV can allow the reducing the dosage of chlorine to a certain extent in the disinfection process. The left part of Fig. 3 is the THMs formation concentration in water samples by only chlorine disinfection (1.2 mg/L, 2.0 mg/L, 2.8 mg/L, and 3.6 mg/L) with reaction after 24 h. The right part is the THMs concentration in water samples after UV radiation followed by 1.2 mg/L initial chlorine solution. As can be seen from Fig. 3, the THMs concentrations were 51.11 μg/L, 60.34 μg/L, 65.45 μg/L, and 72.35 μg/L respectively in water samples chlorinated. The concentration of THMs generated from 64.66 μg/L to 67.97 μg/L in water samples treated by UV irradiation with an average THMs concentration of 66.4 μg/L, which was equivalent to the amount generated at only 2.8 mg/L chlorine. It also increase about 29.9% than the amount at only 2.8 mg/L chlorine and decreased about 8.22% than the amount at only 3.6 mg/L chlorine. But UV radiation had obvious advantages in reducing the species of microorganisms and community complexity in water samples, and low UV dosage showed a very good sterilization effect. Under the experimental conditions, UV had exhibited a good disinfection effect, which can significantly reduce the dosage amount of chlorine needed, thereby reducing THMs formation in the combined disinfection process of UV and chlorine. The concentrations of THMs formation reduced in this study, which was different from previous research findings, mainly because the same concentration of chlorine was added to the water samples with and without UV treatment to explore the formation of THMs in the previous studies. It is reasoned that only separate chemical detection being implemented rather than the additional consideration of inactivation sterilization of UV irradiation, which would reduce the dosage of chlorine in previous processes.

3.4. Influence of UV intensity on the formation of THMs

The formation of THMs in samples under two types of intensity (900 μw/cm^2~500 μw/cm^2) after different doses of UV irradiation at the reaction time of 0.5 h, 5 h, and 24 h are shown in Fig. 4.

The lower UV intensity, the higher concentration of the THMs produces under the same irradiation dosage. The concentration of THMs was almost unanimous under different UV intensity in untreated samples and samples with the highest UV dose (1620 mJ/cm^2). The reason may be that when the UV intensity is small, the oxidized intermediates from organic matter reacted more easily with chlorine under the longer exposure time, even though low energy of irradiation under the same UV irradiation dosage caused residual chlorine decay at a faster rate. And it may also be that higher UV intensity had a better effect on bacteria inactivation in water samples, and reduced the consumption of chlorine.

3.5. Water quality of water samples after UV irradiation

The chlorine decay rate and the amount of THMs formation are not identical in samples after UV irradiation and chlorination followed because of the changes of organic

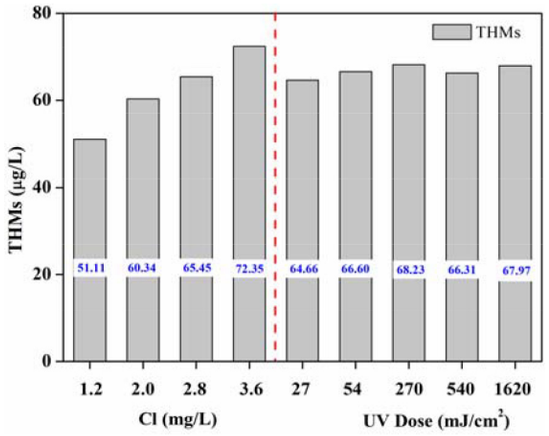

Fig. 3. THMs formation in disinfection process: chlorination only and UV-Cl.

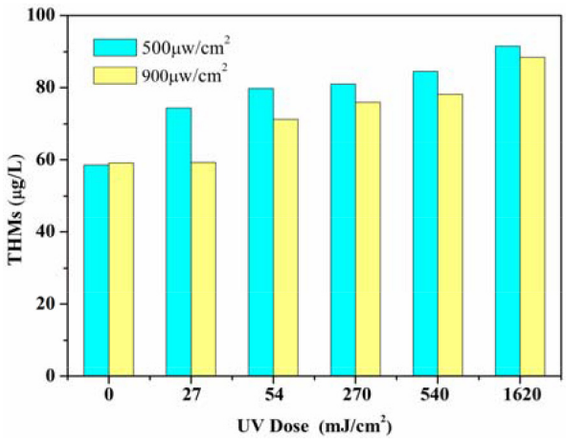

Fig. 4. Influence of UV intensity on the formation of THMs.

matter in different water samples. The changes of organic matter were measured by the three-Dimensional Excitation-Emission Matrix (3DEEM) fluorescence scanning in the water sample after UV irradiation.

Full-wave UV spectra of samples after UV irradiation were measured at the range of 210 nm~300 nm. There is no significant difference between the various water samples according to UV absorbance change tendency (Fig. 5). However, when the value of UV at 1620 mJ/cm^2 as a fixed value, the difference between the benchmark and all absorbance was obtained as the ordinate of Fig. 5b. Fig. 5c is a diagram of each water sample absorbance at a wavelength of 254 nm. UV_{254} may reflect the concentration of organic matter in water to some extent, especially macromolecular, humus, and other various organic compounds containing aromatic hydrocarbon with C=O and conjugated system with C=C or hydroxy, which had strong UV absorption at 254 nm. There is the literature that the value of UV_{254} was higher in water containing macromolecular organic [20].

As can be seen from Fig. 5b, the value of UV absorbance of water samples reduced with the UV radiation doses increasing. The value of UV_{254} in samples is constantly decreasing with the increasing of radiation dosage as shown in Fig. 5c. Compared with the untreated water samples (0.122 cm^{-1}), the value was 0.102 cm^{-1} under the highest UV dosage, which decreased approximately 16.4%. UV_{254} value indicates a lower concentration of organic compounds containing aromatic hydrocarbon in water and the UV radiation oxidized organic matter containing unsaturated double bonds. But the UV_{254} value at 1620 mJ/cm^2 represented that there are a certain amount of aromatic and humic substances in water samples.

By analyzing the excitation (E_x) wavelength and emission (E_m) wavelength of the fluorescence intensity information, the physical and chemical properties of organic matter could be qualitatively and quantitatively described by 3DEEM. Parallel factor analysis (PARAFAC) was used to analyze EEM patterns, which is unique and could reveal non-deceptive information of spectrum by selecting the appropriate number of factors. The EEM fluorescence spectroscopy involved 27 individual emission spectra at sequential 5 nm increments at excitation wavelengths (λ_{ex}) between 220 and 350 nm. The emission wavelength (λ_{em}) range was set from 270 to 460 nm with 0.5 nm increments. The instrumental parameters were excitation as emission slitsat 5 nm, and scan speed at 1200 nm/min. To clearly demonstrate the influence of UV on the fluorescence intensity, fluorescence EEM spectra at each UV dose were carried out to distinguish the chemical behavior of EEM as shown in supplementary Fig. S2. The intensity of dominant EEM peaks decreased with increasing of UV dosage, which indicated that UV treatment could reduce the concentration of organic substances in water.

The appropriate number of components was chosen to be sufficiently high to fully describe the systematic variation in the data of PARAFAC where the core consistency diagnostic score was>80% as shown in Fig. 6. The EEM spectra of the samples after UV irradiation were analyzed by numerically deconvoluting the sample into three EEM components, which are referred to as Component 1, Component 2, and Component 3 (as shown in Fig. 7). According to the dominant EEM peak locations

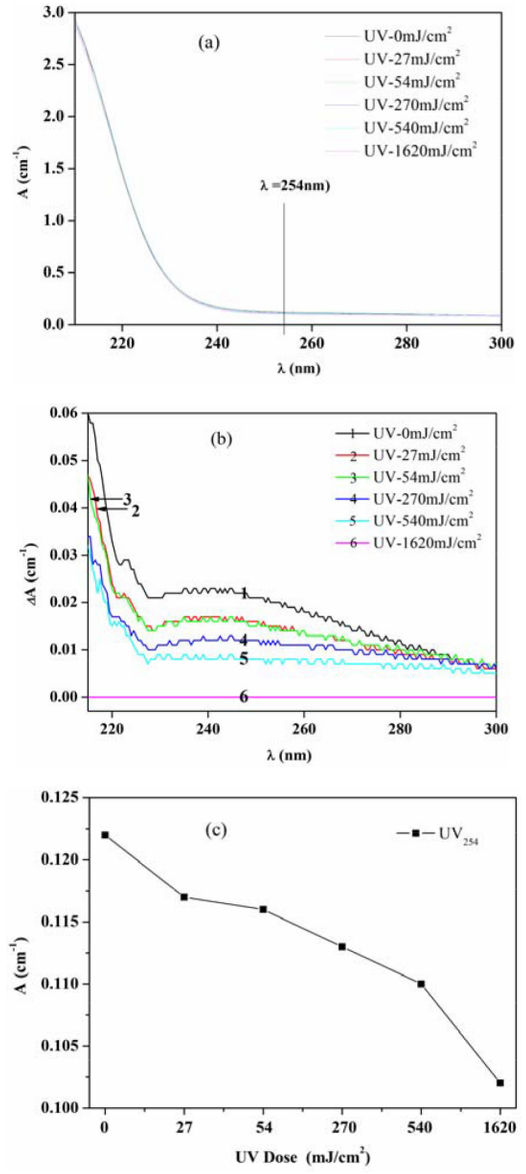

Fig. 5. UV spectrum of samples after UV radiation: (a) UV scanning, (b) The UV absorbance difference and (c) UV_{254}.

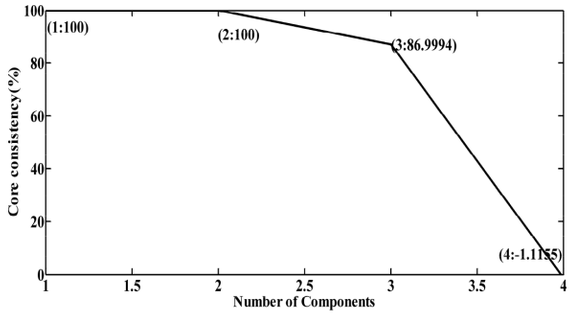

Fig. 6. The appropriate number of components analyzed by PARAFAC.

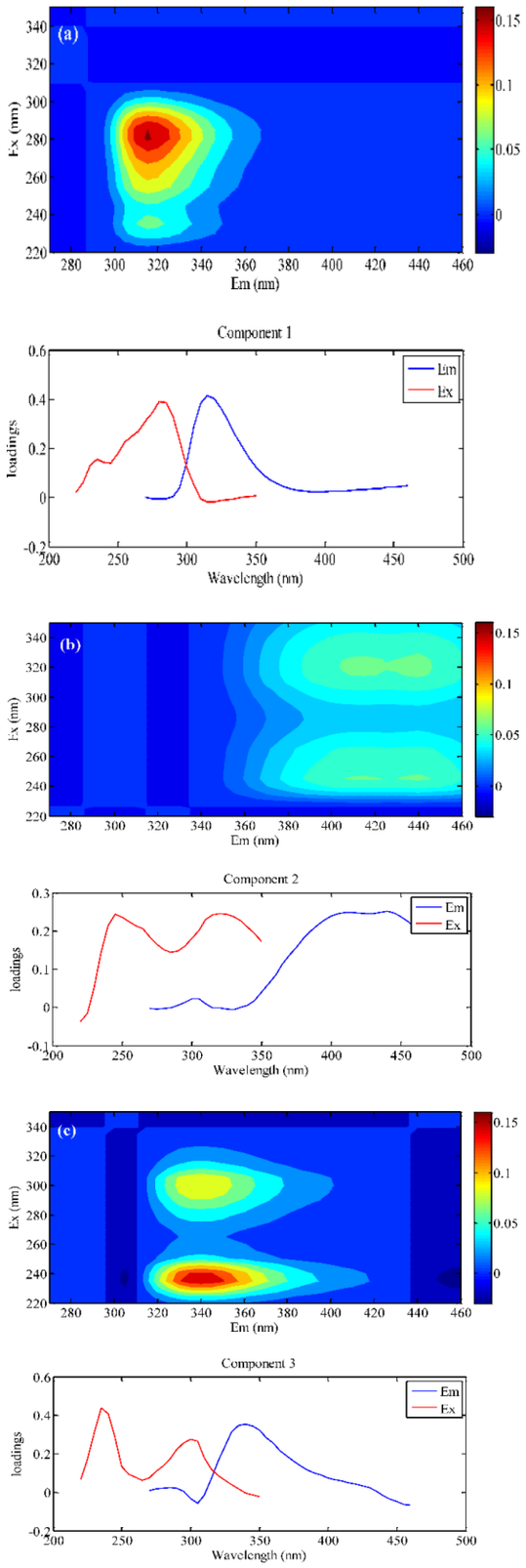

Fig. 7. Three EEM components (a) tyrosine, (b) humic acid and (c) tryptophan.

($\lambda_{ex}/\lambda_{em}$) for these components and the Cobel classification criteria, the three types of components are identified as tyrosine (280 nm/325 nm), humic acid (245 nm (325 nm)/405 nm~445 nm) and tryptophan (240 nm (300 nm)/340 nm) [21,22].

The relative concentration of these components in water samples can be extracted from the PARAFAC analysis after normalization of each component, which represents the real concentration of each PARAFAC component. The results are shown in supplementary Fig. S3. As shown in the figure, the relative concentrations of all three components decreased. The relative concentration levels of the three components in the water sample without UV treatment were 0.3982, 0.2407, 0.238. The relative concentrations at 54 mJ/cm^2 were 0.3517, 0.2693, 0.2156 respectively and the relative concentrations at 540 mJ/cm^2 were 0.1154, 0.2066, 0.102.

So UV treatment can significantly affect the water quality of water samples. The amount of organic matter decreased in terms of the values of UV_{254} and 3DEEM spectrums, and the relative concentration of the three components reduced in water samples after UV irradiation.

4. Conclusions

The effects of UV combined with chlorination disinfection on the quality of filtered water were evaluated in three aspects: 1) the bacterial community structure and the inactivation of microorganisms; 2) the formation of THMs; 3) the changes of NOM structure and water quality.

Compared with chlorine disinfection, UV disinfection showed very good effects in terms of significantly reducing microbial species number and community complexity in water samples. The values of ACE, Chao, Shannon significantly decreased in water samples after UV irradiation, while Simpson slightly increased, which reflected that microbial diversity and abundance significantly decreased in samples after UV irradiation. At the same time, the lower dose (27 mJ/cm^2) exposure to UV showed better disinfection effects than the high concentration of chlorine. After UV disinfection, the dominant species in water samples significantly decreased.

Under the same initial chlorine concentration, the amount of THMs increased with the UV radiation dosage increasing. UV radiation can significantly reduce the chlorine dosage.

At the same dosage, the formation of THMs is inversely proportional to the UV intensity. UV treatment can significantly affect NOM characteristics, and relative concentrations of the substances such as tyrosine, humic acid, and tryptophan. Moreover the substances decreased with the UV radiation doses increasing.

Acknowledgments

This study was kindly supported by the Major Science and Technology Program for Water Pollution Control and Treatment (Grant No.2017ZX07201003), the National Natural Science Foundation of China (No. 51578487, 51778565) and the Zhejiang Provincial Natural Science Foundation of China (No. Y15E080016)

References

[1] S.D. Richardson, M.J. Plewa, E.D. Wagner, R. Schoeny, D.M. Demarini, Occurrence, genotoxicity, and carcinogenicity of regulated and emerging disinfection by-products in drinking water: a review and road map for research, Mutat. Res., 636 (2007) 178–242.

[2] K.P. Cantor, C.F. Lynch, M.E. Hildesheim, M. Dosemeci, J. Lubin, M. Alavanja, G. Craun, Drinking water source and chlorination by products I. Risk of bladder cancer, Epidemiology, 9 (1998) 21–28.

[3] M.B. Toledano, M.J. Nieuwenhuijsen, N. Best, H. Whitaker, P. Hambly, C. de Hoogh, J. Fawell, L. Jarup, P. Elliott, Relation of trihalomethane concentrations in public water supplies to stillbirth and birth weight in three water regions in England, Environ. Health Persp., 113 (2005) 225–232.

[4] N. Corin, P. Backlund, M. Kulovaara, Degradation products formed during UV-irradiation of humic waters, Chemosphere, 33 (1996) 245–255.

[5] J.L. Rand, R. Hofmann, M.Z.B. Alam, C. Chauret, R. Cantwell, R.C. Andrews, G.A. Gagnon, A field study evaluation for mitigating biofouling with chlorine dioxide or chlorine integrated with UV disinfection, Water Res., 41 (2007) 1939–1948.

[6] J.L. Clancy, Z. Bukhari, T.M. Hargy, J.R. Bolton, B.W. Dussert, M.M. Marshall, Using UV to inactivate Cryptosporidium, J. Am. Water Works Ass., 92 (2000) 97–104.

[7] W. Liu, L.-M. Cheung, X. Yang, C. Shang, THM, HAA and CNCl formation from UV irradiation and chlor(am)ination of selected organic waters, Water Res., 40 (2006) 2033–2043.

[8] W.A.M. Hijnen, E.F. Beerendonk, G.J. Medema, Inactivation credit of UV radiation for viruses, bacteria and protozoan (oo) cysts in water: a review, Water Res., 40 (2006) 3–22.

[9] B.A. Lyon, A.D. Dotson, K.G. Linden, H.S. Weinberg, The effect of inorganic precursors on disinfection byproduct formation during UV-chlorine/chloramine drinking water treatment, Water Res., 46 (2012) 4653–4664.

[10] N. Cimetiere, J. De Laat, Effects of UV-dechloramination of swimming pool water on the formation of disinfection by-products: A lab-scale study, Microchem. J., 112 (2014) 34–41.

[11] A.J. Pinto, C. Xi, L. Raskin, Bacterial community structure in the drinking water microbiome is governed by filtration processes, Environ. Sci. Technol., 46 (2012) 8851–8859.

[12] A. Ouali, H. Jupsin, J.L. Vasel, A. Ghrabi, Removal of E. coli and enterococci in maturation pond and kinetic modelling under sunlight conditions, Desal. Water Treat., 53 (2015) 1068–1074.

[13] M. Ben Said, M. Ben Mustapha, A. Hassen, The impact of power supply frequency of a low pressure UV lamp on bacterial viability and activities, Desal. Water Treat., 53 (2015) 1075–1081.

[14] K.M. Ekeren, B.A. Hodgson, S.E. Sharvelle, S.K. De Long, Investigation of pathogen disinfection and regrowth in a simple gray water recycling system for toilet flushing, Desal. Water Treat., 57 (2016) 26174–26186.

[15] S. Eichler, R. Christen, C. Holtje, P. Westphal, J. Botel, I. Brettar, A. Mehling, M.G. Hofle, Composition and dynamics of bacterial communities of a drinking water supply system as assessed by RNA- and DNA-based 16S rRNA gene fingerprinting, Appl. Environ. Microb., 72 (2006) 1858–1872.

[16] T.H. Chiao, T.M. Clancy, A. Pinto, C.W. Xi, L. Raskin, Differential resistance of drinking water bacterial populations to mono chloramine disinfection, Environ. Sci. Technol., 48 (2014) 4038–4047.

[17] Q. Wang, G.M. Garrity, J.M. Tiedje, J.R. Cole, Naive Bayesian classifier for rapid assignment of rRNA sequences into the new bacterial taxonomy, Appl. Environ. Microb., 73 (2007) 5261–5267.

[18] P.D. Schloss, S.L. Westcott, T. Ryabin, J.R. Hall, M. Hartmann, E.B. Hollister, R.A. Lesniewski, B.B. Oakley, D.H. Parks, C.J. Robinson, J.W. Sahl, B. Stres, G.G. Thallinger, D.J. Van Horn, C.F. Weber, Introducing mothur: open-source, platform-independent, community-supported software for describing and comparing microbial communities, Appl. Environ. Microb., 75 (2009) 7537–7541.

[19] W.W. Ben, P.Z. Sun, C.H. Huang, Effects of combined UV and chlorine treatment on chloroform formation from triclosan, Chemosphere, 150 (2016) 715–722.

[20] J.K. Edzwald, Coagulation in drinking water treatment particles, organics and coagulants, Water Sci. Technol., 27 (1993) 21–35.

[21] K.R. Murphy, A. Hambly, S. Singh, R.K. Henderson, A. Baker, R. Stuetz, S.J. Khan, Organic matter fluorescence in municipal water recycling schemes: toward a unified PARAFAC model, Environ. Sci. Technol., 45 (2011) 2909–2916.

[22] J.B. Fellman, M.P. Miller, R.M. Cory, D.V. D'Amore, D. White, Characterizing dissolved organic matter using PARAFAC modeling of fluorescence spectroscopy: a comparison of two models, Environ. Sci. Technol., 43 (2009) 6228–6234.

Supplementary Information

Table S1
Water quality of filtered water

	pH	Temperature ℃	Conductivity (μs/cm)	Turbidity (NTU)	Dissolved O_2 (mg/L)	DOC (mg/L)	UV_{254} (cm^{-1})
Filtered water	7.0–7.9	9.6–21.2	305.2–598.6	0.14–0.17	5.18–5.30	5.101–8.911	0.047–0.102

Table S2
High accuracy and precision in the determination of THMs by head space gas chromatography

	Linear interval	Recovery rate (%)*			
	(μg/L)	0.05 μg/L	0.5 μg/L	5 μg/L	R^2
$CHCl_3$	0.01–20	95.8	96.5	105.4	0.9974
$CHCl_2Br$	0.01–5	99.1	98.7	102.3	0.9995
$CHClBr_2$	0.01–5	94.5	96.3	104.6	0.9973
$CHBr_3$	0.01–20	95.3	93.5	95.6	0.9945

*Recovery rate of 0.05, 0.5, 5 μg/L concentration of the blank recovery rate, each group of experiments were repeated three times, calculated the average value.

Table S3
Identified viable bacteria classes in the water samples

Taxon	Property	Filter-P (%)	Cl-1-P (%)	Cl-2-P (%)	Cl-3-P (%)	Cl-4-P (%)	UV-1-P (%)	UV-2-P (%)	UV-3-P (%)	UV-4-P (%)
Acidimicrobiia	\	0.07	0.12	0.01	0.05	0.07	0.01	0.00	0.00	0.02
Acidobacteria	P	0.94	2.41	0.33	0.52	2.25	0.05	0.64	1.55	0.02
Actinobacteria	P	2.44	2.54	1.23	1.51	1.53	0.67	0.99	0.19	0.08
Alphaproteobacteria	N	33.54	42.95	37.02	47.83	26.95	3.81	28.04	7.92	3.02
Anaerolineae	N	0.02	1.51	0.03	0.00	0.02	0.00	0.10	0.00	0.00
Bacilli	N	0.02	0.21	0.55	0.24	0.52	0.02	0.03	0.00	0.01
Betaproteobacteria	N	46.84	37.24	47.79	41.02	50.58	92.89	45.85	77.76	96.54
Candidate_division_TM7	\	0.33	0.24	2.04	0.18	2.12	0.01	0.01	0.09	0.00
Chlamydiae	N	0.01	0.03	0.00	0.01	0.05	0.00	0.12	0.00	0.00
Cyanobacteria	\	0.14	0.07	0.01	0.04	0.15	0.04	0.07	0.00	0.00
Cytophagia	N	0.60	0.58	0.32	0.20	0.79	0.08	0.05	0.00	0.06
Deltaproteobacteria	N	1.70	0.80	0.39	0.17	0.63	0.12	0.63	0.77	0.00
Flavobacteriia	N	5.95	5.42	6.01	5.84	9.14	1.70	0.64	0.18	0.08
Gammaproteobacteria	N	0.98	0.66	0.77	0.48	1.34	0.33	21.81	9.56	0.13
Gemmatimonadetes	N	0.10	0.20	0.24	0.13	0.22	0.04	0.00	0.01	0.00
Negativicutes	N	0.00	0.00	0.00	0.03	0.63	0.00	0.00	0.00	0.00
Nitrospira	P	0.15	0.21	0.13	0.06	0.05	0.02	0.00	0.00	0.00
Planctomycetacia	P	0.05	0.04	0.01	0.00	0.28	0.02	0.05	0.04	0.00
Sphingobacteriia	N	5.54	3.86	2.63	1.29	1.71	0.14	0.18	1.77	0.03
Others		0.58	0.91	0.49	0.40	0.97	0.05	0.79	0.16	0.01

* P: Positive taxon; N: Negative taxon; \: Not determined.

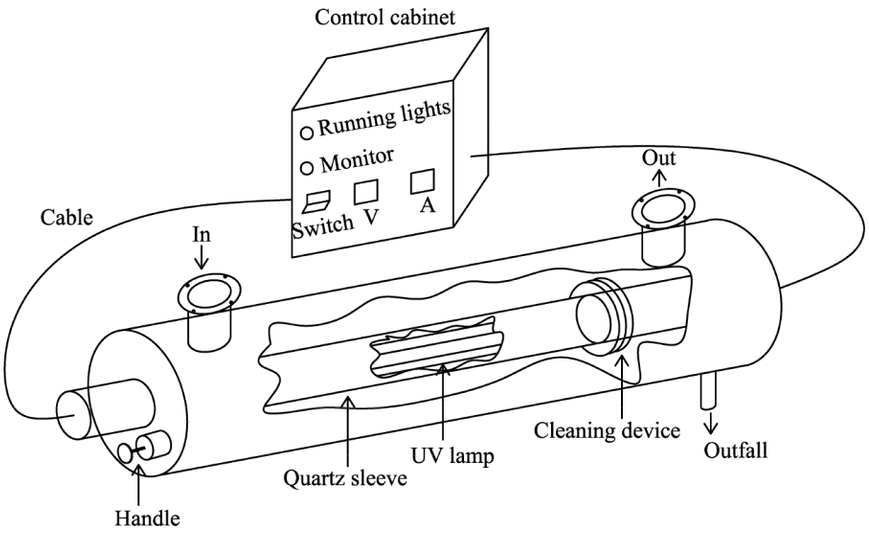

Fig. S1. Graph of ultraviolet disinfection reactor.

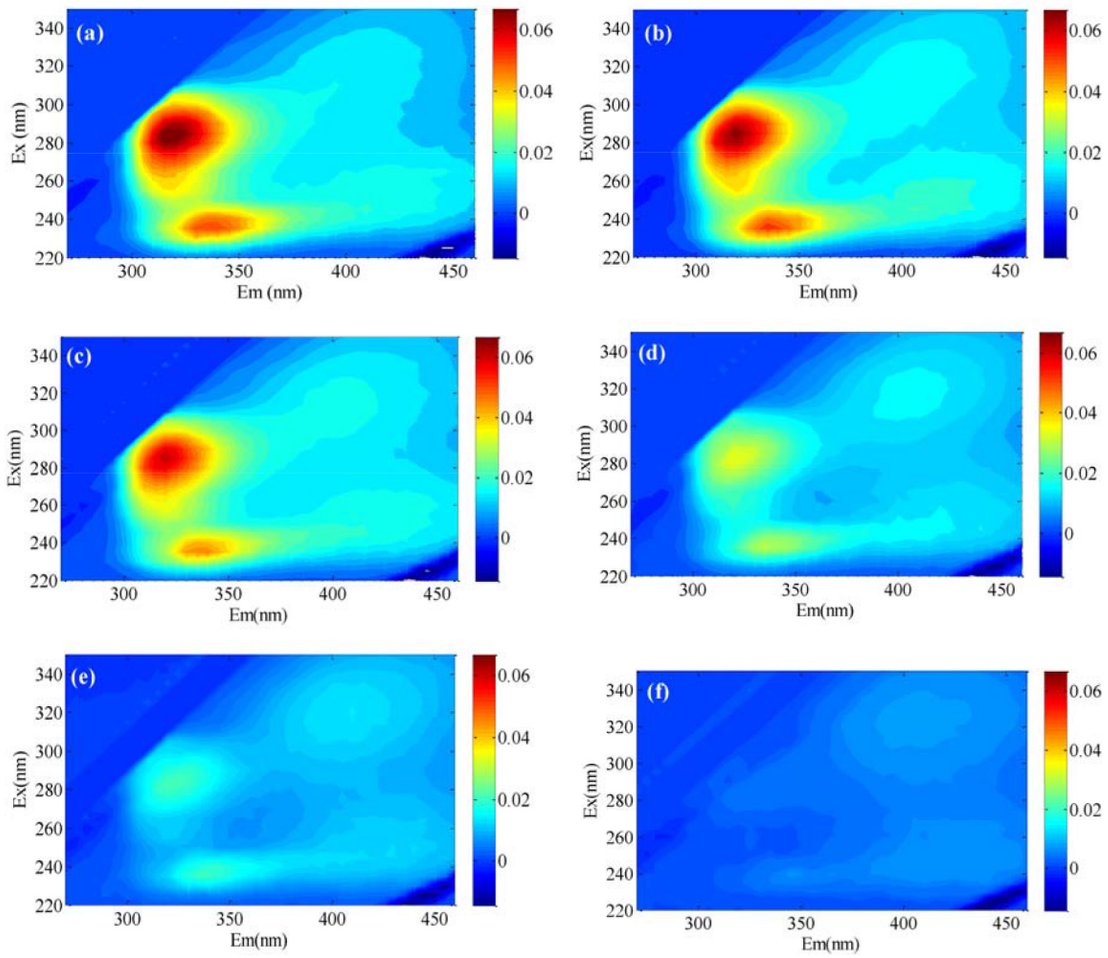

Fig. S2. 3D-EEM spectrums of samples after UV irradiation.

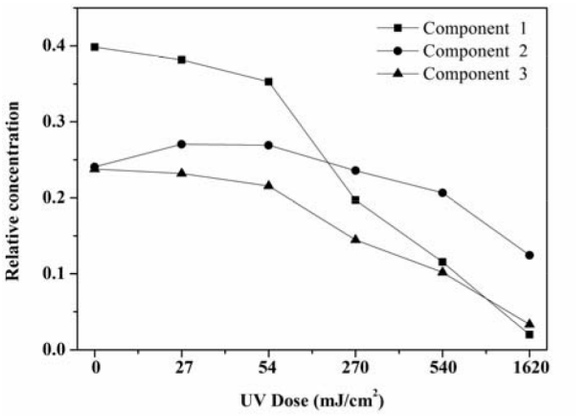

Fig. S3. The relative concentration of these components in water samples after UV irradiation.